Int. J. Heat Mass Transfer. Vol. 32, No. 8, pp. 1389–1400, 1989
Printed in Great Britain

0017–9310/89 $3.00 + 0.00
Pergamon Press plc

Unsteady-state heat and mass transfer in complex-shaped channels

V. M. IYEVLEV, B. V. DZYUBENKO, G. A. DREITSER and V. V. BALASHOV
S. Ordzhonikidze Moscow Aviation Institute, 125871, Moscow, U.S.S.R.

(*Received* 30 *April* 1987)

Abstract—Consideration is given to the problem of unsteady-state heat transfer and working fluid mixing in channels formed by densely packed bundles of oval-shaped coiled tubes with a longitudinally streaming flow and in a plane channel with one-sided heat input. Unsteady-state temperature fields are predicted and experimental results are given for heat and mass transfer processes in bundles of coiled tubes. New laws governing the course of these processes are revealed. It is found that in unsteady-state processes heat transfer coefficients of turbulent diffusion are significantly different from their quasi-stationary counterparts. This difference is determined by the rates of change of boundary conditions—wall temperature and cooling gas flow rate. The explanation for the laws derived is given, as well as recommendations for calculating unsteady-state processes of heat transfer and mixing in channels and determining the limits of applicability of quasi-stationary values for the coefficients of heat transfer and mixing.

1. INTRODUCTION

THE INCREASED interest shown at present to the problem of unsteady-state convective heat transfer in channels is motivated by the great role played by unsteady-state thermal processes in modern power plants, heat exchange and technological equipment and also by high requirements with regard to the accuracy of calculation of these power-intensive facilities. Unsteady-state processes in these apparatus are characterized by rapidly varying parameters which are considered to be controlling in a number of cases. Calculations of unsteady-state thermal processes in power plants, heat exchange apparatus, technological equipment and mains must rely on the results of fundamental investigations into unsteady-state convective heat transfer processes. These investigations are needed to create reliable methods for calculating temperature fields and thermal stresses, heating and cooling of pipelines, mains, elements of power plants and for optimizing these processes, for calculating transient, starting and emergency conditions of operation of various heat exchanging apparatus employed in many areas of technology for developing automatic control systems.

Early investigations, generalized in ref. [1], dealt with unsteady-state heat transfer in circular tubes. Specific features of unsteady-state heat transfer and heat carrier mixing in complex-shaped channels formed by bundles of coiled tubes were the concern of refs. [2, 3].

The present paper suggests results of new experimental investigations of unsteady-state heat and mass transfer in non-circular channels—in a bundle of oval-shaped coiled tubes, in a longitudinally streaming flow, and in a plane channel with heating on one side.

Heat exchange apparatus with coiled tubes can be applied in power engineering and other areas of technology because of their favourable compactness. Plane channels are used in systems for cooling energy generators and internal combustion engines in plate heat exchange apparatus.

2. BUNDLE OF COILED TUBES

2.1. *Prediction of temperature fields and the problems of closing a system of differential equations*

When investigating unsteady-state heat and mass transfer under the conditions of non-uniform heat generation in the bundle cross-section and determining coefficients of turbulent diffusion, use is made of the homogenized medium flow model which represents an actual bundle of coiled tubes and which has proved an efficient means of calculating steady-state temperature fields. The homogenized medium consists of a working fluid and a 'solid phase'. But, while in the case of a steady-state process the one-temperature flow model is used, when calculation of a system of equations [4] yields only the distribution of a working fluid temperature, then in the unsteady-state case, to take into account the thermal inertia of coiled tubes, a two-temperature model is used which also takes into account the change in time of the 'solid phase' temperature. In this case, a system of hydrodynamics and energy equations is solved for a gas flow and a heat conduction equation is solved for a 'solid phase' [2]. When the disturbances of the parameters that determine the flow process are not large and their duration is much in excess of the time of sound wave propagation along the length of the bundle, the gas dynamics equations can be written in quasi-stationary approximation with the continuity equation replaced

NOMENCLATURE

a	thermal diffusivity
c	heat capacity
d	maximum dimension of the oval-shaped tube
d_e	equivalent diameter
d_k	bundle diameter
D_t	effective coefficient of turbulent diffusion
F	cross-sectional area of bundle occupied by tubes
F_f	cross-sectional area of bundle occupied by heat carrier
Fo	Fourier number
Fr_M	dimensionless number characterizing the relationship between inertial and centrifugal forces in a twisting flow
g	acceleration of gravity
G	mass flow rate of working fluid
G_1	mass flow rate of working fluid before disturbance introduction
G_2	mass flow rate of working fluid after disturbance introduction
K	dimensionless coefficient of turbulent diffusion
K_τ	ratio of unsteady-state heat transfer coefficient to its quasi-stationary counterpart
K_G	parameter of dynamic unsteadiness
K_{Tg}	parameter of thermal unsteadiness
l	length of a bundle
Le_T	turbulent Lewis number
m	working fluid-based void content in a bubble
N	heat loading
Nu	Nusselt number
p	static pressure
Pr_T	turbulent Prandtl number
r	radial coordinate
R	gas constant
Re	Reynolds number
q_v	density of volumetric heat generation in the walls of coiled tubes or in a plane channel
q_w	heat flux density on a wall
S	pitch of tube spiral
T	temperature
u, v	velocities
z	longitudinal coordinate.

Greek symbols

α	heat transfer coefficient
κ	relative coefficient of working fluid mixing
λ	thermal conductivity
λ_e	effective coefficient of turbulent diffusion
μ	dynamic viscosity
ν	kinematic viscosity
ν_e	effective coefficient of turbulent viscosity
ξ	coefficient of hydraulic resistance
Π	wetted perimeter
ρ	density
τ	time.

Subscripts

b	bulk mean
f	working fluid
m	mean
M	modified
max	maximum
p	at p = const.
qs	quasi-steady
T	'solid phase'
un	unsteady
w	wall.

by the relation for the working fluid flow rate of the form

$$G(\tau) = 2\pi m \int_0^{r_k} \rho u r \, dr. \quad (1)$$

Here $G(\tau)$ is the known quantity. Then the equation of motion has the form

$$\rho u \frac{\partial u}{\partial z} = -\frac{\partial p}{\partial z} - \xi \frac{\rho u^2}{2d_e} + \frac{1}{r}\frac{\partial}{\partial r}\left(r\rho\nu_e \frac{\partial u}{\partial r}\right). \quad (2)$$

In ref. [2], the heat conduction equation was written for the case when the thermal conductivity coefficient of a 'solid phase' λ_T can be applied as an isotropic coefficient which is independent of directions. In actual fact, this coefficient depends on coordinates, and the heat conduction equation for a 'solid phase' has the form

$$\rho_T c_{pT} \frac{\partial T_T}{\partial \tau} = q_v - \frac{4\alpha m}{(1-m)d_e}(T_T - T) + \frac{1}{r}\frac{\partial}{\partial r}\left(r\lambda_{Tr}\frac{\partial T_T}{\partial r}\right) + \frac{\partial}{\partial z}\left(\lambda_{Tz}\frac{\partial T_T}{\partial z}\right) \quad (3)$$

where λ_{Tr} and λ_{Tz} are the thermal conductivity coefficients of a 'solid phase' in the radial and longitudinal directions, respectively. In view of the fact that the 'solid phase' is uniformly distributed throughout the volume of the shell with an enclosed bundle of coiled tubes, the 'solid phase' temperature T_T is essentially the surface temperature of these tubes at a fixed point in space at a given time τ. Knowing the dis-

tribution of the temperature T_T over the outer surface of the actual tubes, it is possible to solve the problem of determining unsteady-state temperature fields in the wall of the tubes with boundary conditions of the third kind on the inner surface of the tubes. However, when solving the system of equations (1)–(3) and the energy and state equations

$$\rho c_p \frac{\partial T}{\partial \tau} + \rho u c_p \frac{\partial T}{\partial z} + \rho v c_p \frac{\partial T}{\partial r} = \frac{4\alpha}{d_e}(T_T - T) + \frac{1}{r}\frac{\partial}{\partial r}\left(r\lambda_e \frac{\partial T}{\partial r}\right) + \frac{\partial}{\partial z}\left(\lambda_e \frac{\partial T}{\partial z}\right) \quad (4)$$

$$p = \rho R T \quad (5)$$

it is necessary to ensure that the thermoinertial properties of the actual bundle and of the homogenized medium 'solid phase' be the same. It is only in this case that the coincidence of the measured and predicted temperature fields of the fluid and 'solid phase' can be achieved.

In experiments described in ref. [2], the tubes contained quiescent air and their walls were from 0.2 to 0.5 mm thick. Under such conditions there was no convective heat transfer inside the tubes. Therefore, it was possible to use the following calculational schemes for determining the quantities ρ_T, c_T, λ_{Tr} and λ_{Tz}.

Thus, in the calculation of ρ_T the volume which is occupied by the fluid inside the tubes is taken into account

$$\rho_T = \rho_M(1-\varepsilon) + \rho_f \varepsilon \quad (6)$$

where ε is the ratio of the tube flow area to the total area of the tube cross-section.

The thermal conductivity coefficients of the 'solid phase' in the radial and longitudinal directions, λ_{Tr} and λ_{Tz}, respectively, were determined from the equations

$$\lambda_{Tr} = \left[\frac{1-\varepsilon}{\lambda_T} + \frac{\varepsilon}{\lambda_f}\right]^{-1} \quad (7)$$

$$\lambda_{Tz} = \lambda_T(1-\varepsilon) + \lambda_f \varepsilon \quad (8)$$

where λ_T and λ_f are the thermal conductivities of the tube material and of the fluid. These relations take into account the influence of the design of coiled tubes on heat conduction along the bundle 'skeleton', they were derived using the concept of an equivalent thermal conductivity coefficient of a multilayered wall composed of dissimilar materials (the wall and the fluid). The results of numerical experiments with varying values of λ_{Tr} and λ_{Tz} showed that this approach is quite acceptable within the framework of the homogenized model.

The heat capacity of the 'solid phase' was determined from

$$c_T = c_M(1-\varepsilon) + c_f \varepsilon. \quad (9)$$

When the system of equations (1)–(5) was solved numerically, the following boundary conditions were added to it:

at the inlet to the bundle ($z = 0$)

$$\left.\begin{aligned} T_T(r,0,\tau) = T_{Tin}(r,\tau), \quad T(r,0,\tau) = T_{in}(r,\tau), \\ u(r,0,\tau) = u_{in}(r,\tau), \quad p(r,0,\tau) = p_{in}(\tau); \end{aligned}\right\} \quad (10)$$

at the outlet (the condition of the absence of heat transfer)

$$\left.\frac{\partial T_T(r,z,\tau)}{\partial z}\right|_{z=l} = 0, \quad \left.\frac{\partial T(r,z,\tau)}{\partial z}\right|_{z=l} = 0; \quad (11)$$

on the bundle axis (the condition of axial symmetry)

$$\left.\frac{\partial T_T(r,z,\tau)}{\partial r}\right|_{r=0} = 0, \quad \left.\frac{\partial T(r,z,\tau)}{\partial r}\right|_{r=0} = 0, \quad \left.\frac{\partial u}{\partial r}\right|_{r=0} = 0; \quad (12)$$

on the outer boundary of the bundle

$$-\lambda_{Tr}\left.\frac{\partial T_T(r,z,\tau)}{\partial r}\right|_{r=r_K} = 0, \quad -\lambda_e \left.\frac{\partial T(r,z,\tau)}{\partial r}\right|_{r=r_K} = 0, \quad \left.\frac{\partial u}{\partial r}\right|_{r=r_K} = 0. \quad (13)$$

Initial conditions were obtained by solving an unsteady-state problem at time $\tau = 0$. For the solution of the system of equations (1)–(5) with boundary conditions (10)–(13), the quantities accompanying the derivatives were preliminarily averaged depending on the differentiation coordinates, taken outside the differentiation sign, and then refined in iteration cycles.

The heat transfer and energy equations were solved by the alternating-direction method. Numerical analogues of the equations were broken down into an implicit scheme and were solved by the factorization method. The motion and continuity equations were also solved by this method. Thus, just as in ref. [2], the solution was split into successive steps—solution of heat transfer equations (3) and (4) and simultaneous solution of motion and continuity equations (2) and (1), which were thereafter linked via the equation of state, equation (5), and iteration cycles.

An algorithm to generate the solution was realized in the form of a computational programme coded in Fortran for a BESM-6 computer [6].

To close the system of equations (1)–(5), use is made of experimental values of the heat transfer coefficient α, effective coefficients of thermal conductivity λ_e and viscosity ν_e, as well as of the hydraulic resistance coefficients ξ. Taking, just as in ref. [2], the turbulent Prandtl and Lewis numbers equal to unity, $Pr_T = 1$ and $Le_T = 1$, it is sufficient to find from experiment the dimensionless equivalent coefficient of turbulent diffusion

$$K = \frac{D_t}{ud_e} \tag{14}$$

because $\lambda_e = D_t \rho c_p$ and $\nu_e = D_t$.

Coefficient K is determined by comparing the measured and predicted temperature fields of the working fluid at each instant of time τ. In this case it is determined in which way the coefficient K depends on the similarity criteria.

The specific features of heat and mass transfer in a bundle of coiled tubes are dictated both by the features of bundle construction and by the influence of the unsteadiness effects. As is known [4], the twisting of a flow in a bundle of coiled tubes is determined by the relative pitch s/d by

$$Fr_M = s^2/dd_c \tag{15}$$

which characterizes the ratio between inertia and centrifugal forces acting on the flow in its twisting. The number Fr_M represents a complex geometric characteristic of the bundle. The smaller the s/d (or Fr_M), the greater the rate of flow twisting. The twisting of the flow gives rise to fields of transverse velocity vector components in the bundle cross-section. In this case the wall layer is agitated to a greater degree than the core of the flow. Thus, the ratio between the turbulization levels in these flow regions for a bundle with $Fr_M = 178$ is approximately twice as high as a similar ratio for a circular tube [4].

This feature of heat and mass transfer in a bundle of coiled tubes seems to be the major factor in the enhancement between the wall layer and the flow core. The generation of turbulence in the wall layer by flow twisting and intensive convective exchange by portions of liquid between the wall layer and the flow core can enhance the influence of unsteadiness on the flow structure.

In addition to Fr_M, the similarity criteria include the Reynolds number

$$Re = \frac{u_m d_e \rho}{\mu} \tag{16}$$

and also the working fluid-based void content of the bundle which characterizes the fraction of the area of radial cross-sections over which the working fluid contacts on the boundaries of the adjacent cells of the bundle [4]

$$m = F_f/F_\Sigma \tag{17}$$

where $F_\Sigma = F_f + F$ is the cross-sectional area of the bundle. Then, the criterion connection for the stabilized value of K_{qs} for the steady-state regime takes the form

$$K_{qs} = K(Re, Fr_M, m). \tag{18}$$

The specific features of heat and mass transfer under unsteady-state conditions of the occurrence of processes are also due to changes in the turbulent structure of flow in its wall region. In this case, the mechanism of unsteady-state heat and mass transfer in this region is governed by the processes which are typical of unsteady-state heat transfer in circular tubes [1].

Once the analysis is based on the methods of the similarity theory, then it is possible, from the complete set of equations describing the unsteady-state flow of liquid with simultaneous heat transfer, to determine the Fourier number (the criterion of thermal homogeneity) which characterizes the relationship between the rate of change in the temperature field of the working fluid, its physical properties and dimensions of the flow region

$$Fo_h = \frac{\lambda_h \tau}{c_p \rho_h d_k^2} \tag{19}$$

and which is the decisive criterion for describing unsteady-state processes with the aid of dimensionless equations.

The controlling parameter in the case of a change in the working fluid flow rate at a constant heat flux density is taken to be the ratio between the working fluid flow rates before and after the introduction of disturbance, G_2/G_1. The dimensionless non-stationary effective coefficient of turbulent diffusion will be determined by the following criterion connection:

$$K_{un} = K(Re, Fr_M, m, Fo_h, G_2/G_1). \tag{20}$$

It may be more convenient to represent experimental data on unsteady-state heat and mass transfer with the aid of the concept of the relative coefficient of mixing $\kappa = K_{um}/K_{qs}$, where K_{qs} is the quasi-stationary value of the dimensionless effective coefficient of turbulent diffusion. Then the dimensionless equation will have the form

$$\kappa = \kappa(Fo_h, Fr_M, Re, G_2/G_1). \tag{21}$$

This equation does not include the working fluid-based void content of the bundle because this quantity influences identically the coefficients K_{un} and K_{qs} for the bundle of coiled tubes under consideration. The dimensionless equation (21) can also involve other parameters that take into account the effect of unsteady-state boundary conditions on κ.

2.2. *Unsteady-state heat and mass transfer on a change in the heat flux density. Generalization of experimental data obtained*

An experimental investigation of unsteady-state heat and mass transfer processes was carried out on bundles made of 127 coiled tubes with the relative pitches of tube spirals $s/d = 12$ and 6.1 (which correspond to $Fr_M = 220$ and 57), with electrical power being applied to 37 central tubes, within the Reynolds number range $Re = 3.5 \times 10^3$–1.75×10^4, maximum values of the heat flux density derivative with respect to time $(\partial N/\partial \tau) = 0.615$–$3.64$ kW s^{-1} and of time

delays in heat loading supply $\tau_0 = 1$–6.5 s (Fig. 1). The experiments were run both in the case of rapid and slow achievement of steady-state operational conditions. Models were made of the processes of start-up, transition from one to another operational regime and of the apparatus stoppage. The working fluid temperature fields were measured at the outlet of the bundle by a rack of ten chromel–alumel thermocouples. A special automatic system was used to control the apparatus, to gather and process experimental data for the unsteady-state process of mixing and heat transfer [2, 3]. The temperature fields measured for different instants of the unsteady-state heat transfer process were compared, by the least squares method, with temperature fields obtained in solving the system of equations (1)–(5) with different prescribed values of K_{un}. Figure 2 presents the predicted and measured temperature distributions for different instants of time for one of the operational regimes of the bundle with $Fr_M = 220$. Analogous temperature fields for the other operational regimes were given in refs. [2, 3]. The fitting of the data of refs. [2, 3] with the new results made it possible to reveal the influence of the derivative $(\partial N/\partial\tau)_{max}$ on the coefficient $\kappa = K_{un}/K_{qs}$ and to correlate experimental data for the case of $Fr_M = 220$ and heat flux density increasing at the above-mentioned rate by the relation (Fig. 3)

$$\kappa = K_{un}/K_{qs} = 0.307\times10^{-4}Fo^{-2} - 0.226\times10^{-2}Fo^{-1} + 0.91 \quad (22)$$

where

$$Fo = \frac{\lambda_b(\tau-\tau_0)}{c_p\rho_b d_K^2}[a + b(\partial N/\partial\tau)_{max}]. \quad (23)$$

The coefficients $a = 0.043$ and $b = 0.263$ s kW^{-1}

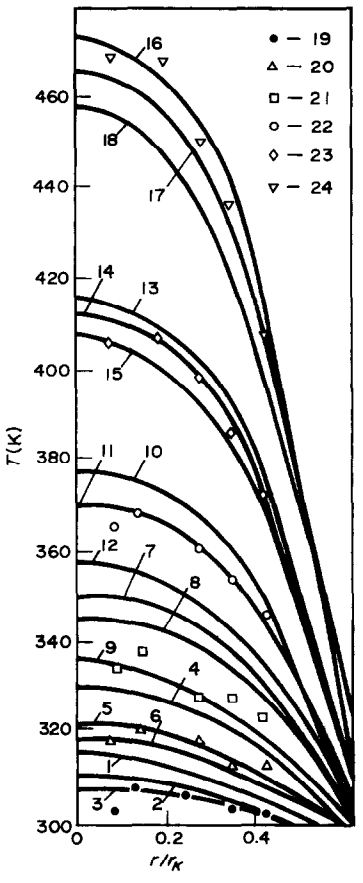

FIG. 2. Working fluid temperature fields in the outlet section of a bundle with $s/d = 12$ ($Fr_M = 220$) at $Re = 3.5\times10^3$: 1–18, calculation; 1–3, $\tau = 16.85$ s, $K = 0.1$, 0.2, 0.3, respectively; 4–6, same for $\tau = 20.8$ s; 7–9, same for $\tau = 24.8$ s; 10–12, $\tau = 32.8$ s, $K = 0.06$, 0.1, 0.2; 13–15, $\tau = 44.8$ s, $K = 0.045$, 0.06, 0.08; 16–18, same for $\tau = 72.8$ s; 19–24, experimental data for $\tau = 16.8$, 20.8, 24.8, 32.8, 44.8, 72.8 s, respectively.

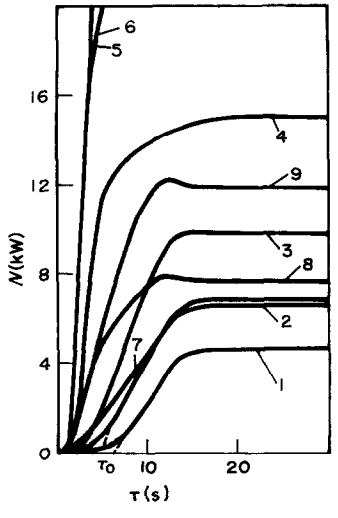

FIG. 1. Change in time in energy generation: 1–6, for a bundle of coiled tubes with $Fr_M = 220$ and for $Re = 3.5\times10^3$, 6.4×10^3, 8.8×10^3, 8.9×10^3, 1.36×10^4, 1.75×10^4, respectively; 7–9, same for a bundle with $Fr_M = 57$ and for $Re = 5.1\times10^3$, 8.9×10^3, 1.25×10^4.

characterize the aspects of heat power when the bundles studied reach the unsteady-state operational regime (Fig. 1). For the bundle with $Fr_M = 57$ and increasing heat power, the influence of the derivative $(\partial N/\partial\tau)_{max}$ on κ in the case of rapid and slow variations of power and during the transition from one regime to another is analogous to the case with $Fr_M = 220$. Then, the experimental data for $Fr_M = 57$ can be correlated as (Fig. 3)

$$\kappa = 0.114\times10^{-4}Fo^{-2} - 0.1053\times10^{-2}Fo^{-1} + 1.024 \quad (24)$$

indicating a speeding up in the equalization of temperature irregularities in the working fluid flow with a decreasing Fr_M. Thus, an increase in flow twisting leads to an increase of the level of turbulence in the wall layer in unsteady-state heating thus intensifying the exchange processes between the wall layer and the flow core. The influence of Re on κ is not observed in the experiments. Experimental data for the bundles

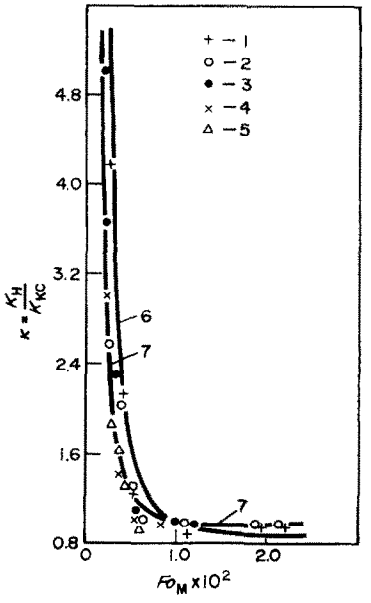

FIG. 3. The dependence of κ on Fr_M: 1–5, experimental data for $Fr_M = 57$ at $Re_b = 1.25 \times 10^4$, $(\partial N/\partial\tau)_{max} = 1.212$ kW s^{-1}; $Re_b = 8.9 \times 10^3$, $(\partial N/\partial\tau)_{max} = 1.212$ kW s^{-1}; $Re_b = 5.1 \times 10^3$, $(\partial N/\partial\tau)_{max} = 0.622$ kW s^{-1}; $Re_b = 5.1 \times 10^3$, $(\partial N/\partial\tau)_{max} = 0.115$; $Re_b = 5.1 \times 10^3$, $(\partial N/\partial\tau)_{max} = 0.35$ kW s^{-1}, respectively; 6, plot for $Fr_M = 57$ (24).

within the ranges $Fr_M = 57$–220 and $Fo = 0.25 \times 10^{-2}$–1×10^{-2} can be generalized by a single relation of the form

$$\kappa = (0.114 \times 10^{-4} Fo^{-2} - 0.1053 \times 10^{-2} Fo^{-1} + 1.024) + \frac{Fr_M - 57}{45.4 \times 10^6 Fo_M^2 - 18.88 \times 10^4 Fo_M + 245}. \quad (25)$$

The investigations of unsteady-state heat and mass transfer with an increasing thermal load showed that the change in time of the working fluid temperature distributions (Fig. 2) and accompanying variations of the effective coefficient of diffusion K_{un}, which characterizes the transfer properties of the flow, were due to the influence of unsteady-state boundary conditions. The observed rearrangement of temperature fields and pronounced enhancement of heat and mass transfer at the first instants of time can be attributed to the change in the turbulent flow structure during unsteady-state heating of the bundle.

When the power of thermal loading decreases, κ is much smaller than unity at the first time instants, i.e. the non-stationary value of the diffusion coefficient K_{un} is smaller than its quasi-stationary value K_{qs} [2, 3]. The present paper analyses experimental data obtained for this type of unsteadiness over the ranges: $Re = 5.1 \times 10^3$–1.25×10^4, $|(\partial N/\partial\tau)_{max}| = 1.075$–$10$ kW s^{-1}, and $Fr_M = 57$ and 220. The analysis involves not only regimes in which the thermal loading power decreases to zero, but also the transition from one to another operational regime with a smaller heat load (Fig. 4). The variation of K_{un} with Fo, determined from equation (23), for the operational regimes considered is well described by the following equation valid for $Fo \leqslant 1.4 \times 10^{-2}$:

$$\kappa = 0.454 \times 10^{-5} Fo^{-2} - 3.86 \times 10^{-3} Fo^{-1} + 1.28. \quad (26)$$

Equation (26) agrees well with experimental data (Fig. 5) for both the bundle with $Fr_M = 220$ and the bundle with $Fr_M = 57$.

The relation

$$\kappa = 0.454 \times 10^{-5} Fo_b^{-2} - 3.86 \times 10^{-3} Fo_b^{-1} + 1.24 \quad (27)$$

suggested in refs. [2, 3] is valid only in the case of a sudden decrease in the power of heat loading to zero at $|(\partial N/\partial\tau)_{max}| = 7.5$–$10$ kW s^{-1} (Fig. 5).

Thus, the criterion Fr_M exerts different effects on K_{un} in the cases of increasing and decreasing heat loads. In unsteady-state heating of tubes temperature irregularities equalize more rapidly with an increase in Fr_M due to additional flow turbulization in the wall layer, whereas during a decrease in heat loading the influence of Fr_M on κ is not observed.

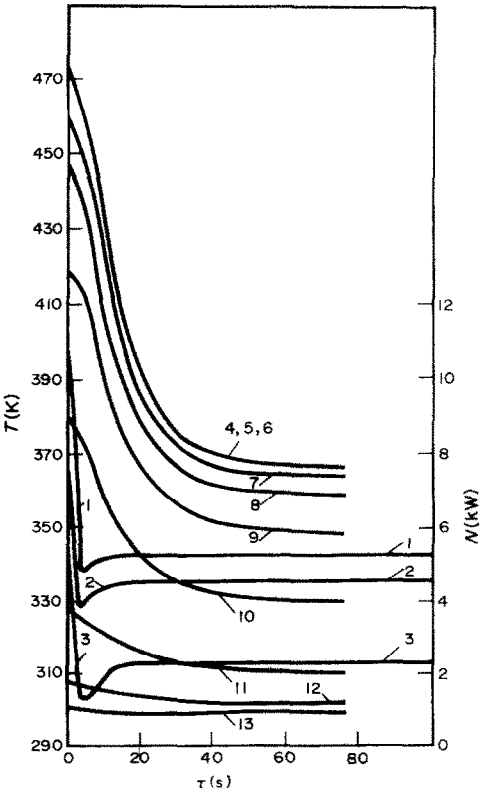

FIG. 4. Variation of heat loading and of working fluid temperature in time on transition to the other, lower, operational regime: 1–3, change in loading at $Re = 1.25 \times 10^4$, 8.9×10^3, 5.1×10^3, respectively; 4–13, change in the working fluid temperature for $Re = 1.25 \times 10^4$ at $r/r_K = 0.073$, 0.128, 0.193, 0.265, 0.334, 0.408, 0.479, 0.624, 0.770, 0.916, respectively.

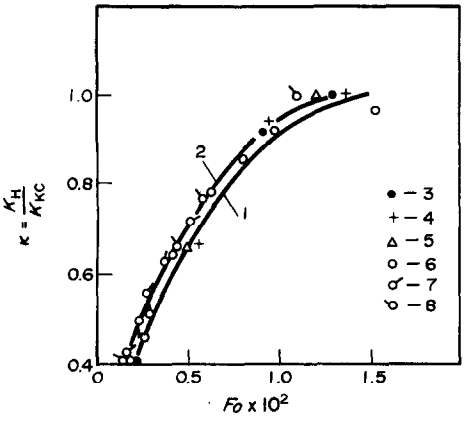

FIG. 5. The dependence of κ on Fourier number on a decrease in heat loading: 1, relation (27); 2, relation (26); 3–5, experimental data for bundle with $Fr_M = 220$ at $Re = 8.9 \times 10^3$ and $|(\partial N/\partial\tau)_{max}| = 7.5$ kW s^{-1}, $Re = 1.36 \times 10^4$ and $|(\partial N/\partial\tau)_{max}| = 10$ kW s^{-1}, $Re = 1.75 \times 10^4$ and $|(\partial N/\partial\tau)_{max}| = 10$ kW s^{-1}, respectively; 6, experimental data for $Fr_M = 57$, $Re_b = 1.25 \times 10^4$ and $|(\partial N/\partial\tau)_{max}| = 1.875$ kW s^{-1}; 7, same at $Re = 8.9 \times 10^3$ and $|(\partial N/\partial\tau)_{max}| = 1.175$ kW s^{-1}; 8, same at $Re = 5.1 \times 10^3$ and $|(\partial N/\partial\tau)_{max}| = 1.075$ kW s^{-1}.

2.3. *Unsteady-state heat transfer during a change in the working fluid flow rate. Generalization of experimental data*

The influence of acceleration and deceleration of the working fluid flow at a constant density of heat flux power supplied to 37 central coiled tubes of the bundle of 127 tubes was studied experimentally over the range $G_2/G_1 = 0.594$–1.77 at $Fr_M = 57$ and 220. The change of the working fluid flow rate in time was achieved with the aid of a device operating on the principle of a camera shutter [5]. Experimental data were processed following the technique described in Section 2.1. The processing revealed new trends in the unsteady-state heat and mass transfer and in the type of unsteadiness considered. It was found that in the case of working fluid acceleration and constant heat loading a decrease was observed in the working fluid temperature in time. Then κ varies as a function of Fourier number Fo_b in the same way as in the case of decreasing heat load (Section 2.2), i.e. at the first instant of time κ decreases steeply (Fig. 6) and then, with an increase of Fo_b, it tends to unity ($K_{un} \to K_{qs}$). Thus, for the type of unsteadiness considered the main influence on K_{un} is exerted not by the mechanism of flow acceleration, which, by analogy with circular tubes, should have led to an increase of K_{un} [1] at $T_w = \text{const.}$, but rather by the thermal inertia of tubes. In the case at hand the thermal inertia of tubes leads to a change in time of the temperature fields of the working fluid similar to the variation on a decrease in heat load (Fig. 4) when a decrease of K_{un}, as compared with K_{qs}, is observed at the first instant of time, with $K_{un} = K_{un}(Fo_b, G_2/G_1)$. In this case, the experimental data are well correlated by (Fig. 6)

$$\kappa = AFo_b^n + c \tag{28}$$

where A, c and n depend on the ratio G_2/G_1 (Table 1). For the case of low acceleration equation (28) is obtained for $\kappa \leqslant 1$.

The character of the change of κ with G_2/G_1 at different Fo_b for the case of flow acceleration can be illustrated by Fig. 7 showing the plots of

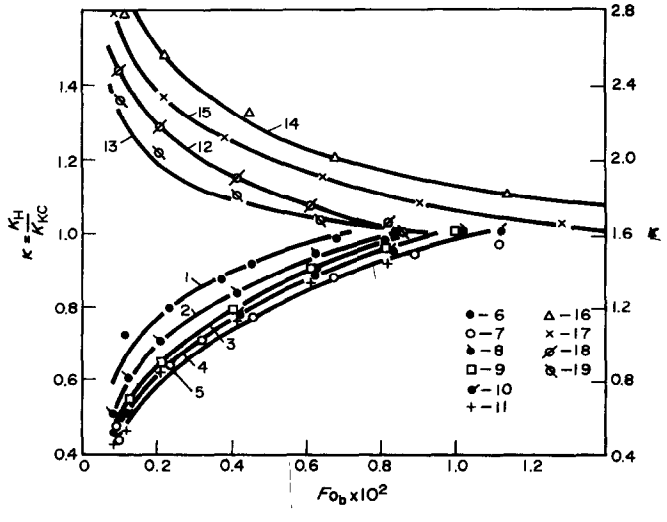

FIG. 6. Comparison of experimental data on the relative mixing coefficient κ with interpolational relations at different Fr_M and flow rate ratios G_2/G_1: 1–5, relation (28) at $G_2/G_1 = 1.62$, 1.68, 1.71, 1.73, 1.77, respectively; 6, 7, experimental data for $Fr_M = 57$ and $G_2/G_1 = 1.62$, 1.77, respectively; 8–11, same for $Fr_M = 220$ at $G_2/G_1 = 1.68$, 1.71, 1.73, 1.77, respectively; 12, 13, relation (28) for $Fr_M = 220$, at $G_2/G_1 = 0.594$ and 0.613, respectively; 14, 15, same for $Fr_M = 57$ at $G_2/G_1 = 0.61$ and 0.665, respectively; 16, 17, experimental data for $Fr_M = 57$ at $G_2/G_1 = 0.61$ and 0.665; 18, 19, same for $Fr_M = 220$ at $G_2/G_1 = 0.594$ and 0.613.

Table 1. The values of A, c and n for the case of flow acceleration

Ordinal No.	G_2/G_1	A	n	c	Fr_M
1	1.62	3.89	0.0764	−1.66	57
2	1.68	3.846	0.0966	−1.425	220
3	1.71	3.758	0.240	−0.210	220
4	1.73	3.758	0.240	−0.235	220
5	1.77	3.758	0.2476	−0.221	57220

$$\kappa = a\left(\frac{G_2}{G_1}\right)^2 + b\left(\frac{G_2}{G_1}\right) + c \qquad (29)$$

where a, b and c depend on Fo_b (Table 2). Equation (29) is obtained for $\kappa \leqslant 1$.

It is seen that the difference of K_{un} from its quasi-stationary counterpart increases with G_2/G_1. There is virtually no influence of Fr_M on κ, i.e. within the range $Fr_M = 57$–220 attained in the experiment Fr_M exerts the same effect on K_{un} and K_{qs}.

In the case of the working fluid flow deceleration (decrease of its flow rate) and at $N = \text{const.}$ K_{un} increases steeply at the first instant of time, then decreases smoothly and tends to the quasi-stationary value K_{qs}. Consequently, for this type of unsteadiness too, the main effect on K_{un} is exerted not by the flow deceleration due to a decrease in the working fluid flow rate (which should have been observed in experiments with $T_w = \text{const.}$ by analogy with circular tubes [1]), but rather by the thermal inertia of tubes which vary in time the working fluid temperature fields in the same way as in the case of an increase in heat loading at a constant working fluid flow rate (Section 2.2). Experimental data for the case of the working fluid flow deceleration (Fig. 6) are also well correlated by the relation of the form of equation (28), but the quantities A, c and n are functions not only of the ratio G_2/G_1, but also of Fr_M (Table 3). In the case of flow deceleration equation (28) is derived for $\kappa \geqslant 1$.

Here, the influence of the ratio G_2/G_1 and of Fr_M on κ is much stronger (Fig. 7(b)) than in the case of an increase of the working fluid flow rate. The influence of Fr_M on the coefficient κ is more substantial than in the case of an increase of heat loading at a constant working fluid flow rate (Fig. 3).

The revealed effects, associated with the influence of the considered types of unsteadiness on the process of working fluid mixing in bundles of coiled tubes, are favourable from the viewpoint of the efficiency of heat exchangers and apparatus with coiled tubes. Thus, on an increase in heat loading at a constant working fluid flow rate or on a substantial decrease in the working fluid flow rate at $N = \text{const.}$—the case possible in emergency situations due to the breakage of pipelines and to the working fluid loss—an increase of κ is observed, i.e. the process of mixing is enhanced as well as the equalization of the nonuniformities of the working fluid temperature fields in a bundle of coiled tubes thus facilitating the thermal operation of the apparatus. When heat loading decreases or the working fluid flow rate increases at $N = \text{const.}$, a decrease of κ and deterioration of fluid mixing at the first instants of time are not reflected in the heat exchanger efficiency due to a noticeable decline in the working fluid mean mass temperature.

2.4. *Unsteady-state heat transfer. Generalized relations*

The unsteady-state heat transfer in bundles of coiled tubes was investigated at a constant airflow rate and step-wise varying electrical loading over the ranges: $Re_b = 5\times10^3$–5×10^4; $T_w/T_b = 1$–1.4; $\partial T_w/\partial\tau = -50$ to $50\ \text{K s}^{-1}$; $z/d_e = 7$–167. The experimental data were generalized by the following equations (Fig. 8):

for an increasing heat flux

$$K_\sigma = \frac{Nu_{un}}{Nu_{qs}} = 1 + (K_{Tq}\times10^5)\frac{2.4}{(T_w/T_b)^{6.2}}; \qquad (30)$$

for a decreasing heat flux

$$K_\alpha = 1 - 0.42[1 - \exp(1.9K_{Tq}\times10^5)]. \qquad (31)$$

It turned out that with an increasing heat flux $K_\alpha = 2$–3 and with a decreasing heat flux $K_\alpha = 0.5$–0.6 at the first instant of time. As the wall temperature is

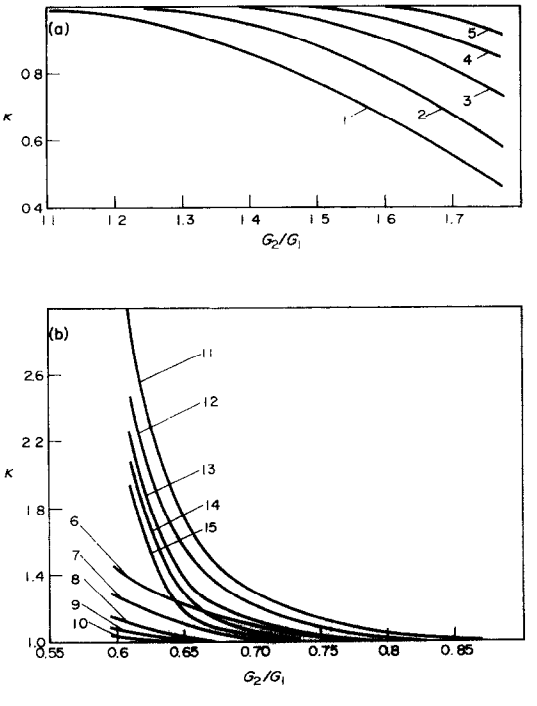

FIG. 7. The influence of the ratio between the working fluid flow rates G_2/G_1 on κ: (a) 1–5, working fluid flow acceleration for bundles with $Fr_M = 57$–220 and for $Fo = 0.1\times10^{-2}$, 0.2×10^{-2}, 0.4×10^{-2}, 0.6×10^{-2}, 0.8×10^{-2}; (b) 6–10, flow deceleration for bundles with $Fr_M = 220$ and for the same Fo; 11–15, same as for $Fr_M = 57$.

Table 2. The values of a, b and c for the case of flow acceleration

Ordinal No.	$Fo_b \times 10^2$	a	b	c
1	0.1	−0.85	1.62	0.27
2	0.2	−1.08	2.435	−0.337
3	0.4	−1.12	2.845	−0.785
4	0.6	−1.235	3.395	−1.3
5	0.8	−1.275	3.79	−1.8

Table 3. The values of A, c and n for the case of flow deceleration

Ordinal No.	Fr_M	G_1/G_2	A	n	c
1	57	0.61	0.309	−0.3	0.589
2	57	0.665	2.344	−0.0639	−2.088
3	220	0.594	2.213	−0.0631	−1.98
4	220	0.0613	0.00589	−0.62	−0.90

stabilized, K_α and $\kappa \to 1$. At the same values of the unsteadiness parameter

$$K_{Tg} = \frac{\partial T_w}{\partial \tau} \frac{1}{T_w} \sqrt{\left(\frac{\lambda_b}{c_p g \rho_b u_b}\right)} \tag{32}$$

the difference of K_α from 1 is higher in a bundle of coiled tubes than in a circular tube [1].

The data obtained for K_α and κ make it possible to calculate temperature fields in a bundle of coiled tubes with non-uniform heat generation field using the system of equations (1)–(5).

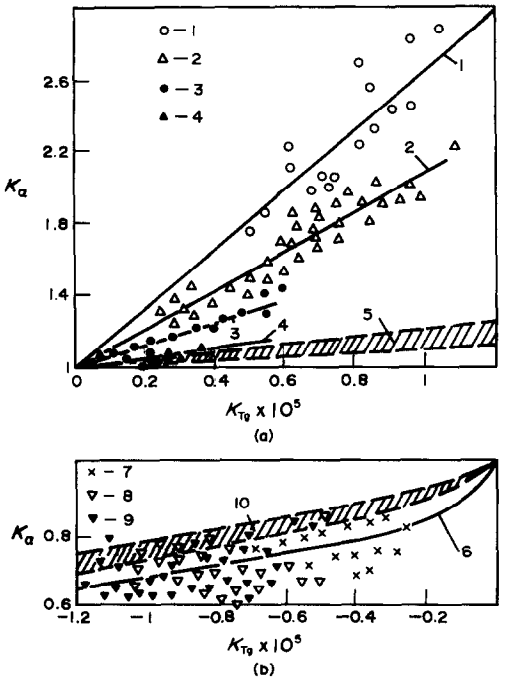

FIG. 8. The dependence of K_α on K_{Tg} for an increasing (a) and decreasing (b) heat loading for bundles of coiled tubes: 1–4, bundles for T_w/T_b = 1–1.1, 1.1–1.2, 1.2–1.3, 1.3–1.4, at $Re_b = 1 \times 10^4$–5×10^4; 5, 10, tube for $Re_b = 1 \times 10^4$–5×10^4; 6, relation (31) for bundles; 7–9, bundles for T_w/T_b = 1.1–1.2, 1.2–1.3, 1.3–1.4 at $Re_b = 1 \times 10^4$–5×10^4.

3. PLANE CHANNEL

The investigation reported in the present paper was concerned with unsteady-state heat transfer in plane channels heated from one side. Experiments were carried out both in a channel with simultaneous formation of thermal and hydraulic initial segments, when the start of heating coincides with the inlet section of the channel (Section No. 1), and in a channel with a thermal initial segment, when the heated wall is located under the conditions of a hydraulically stabilized flow (Section No. 2).

Test Section No. 1 consisted of two thick-wall (steel) plates and two textolite inserts, had a flow area of 40×7 mm and was 300 mm long. Midway between these plates there were two stainless steel, 0.2 mm thick, 40 mm wide and 230 mm long plates sandwiched with 1.6 mm thick glass cloth. The plates were welded to copper busbars and were heated by passing a low-voltage current. A spring facility ensured independent pull of both plates on their expansion. Thus two plane channels with one-sided heating were formed that had a flow area of 40×2.5 mm and a length of 230 mm. This construction made it possible to virtually exclude heat losses.

Section No. 2 had the same dimensions of the heated part of the channel as Section No. 1, but there was a non-heated 350 mm long segment ahead of the heating element.

The following parameters were measured in experiments: the voltage drop and strength of the current passing through the test section, the inner surface temperature of plates at 12 points, the temperature of the non-heated surfaces at 12 points, the flow temperature at the inlet and exit from the test section, the cooling airflow rate, and air pressure at the inlet and outlet.

Investigation was concerned with unsteady-state thermal processes caused by an abrupt change of heat generation in the channel walls at a constant flow rate of the cooling air and by a change in the flow rate at a constant wall temperature.

The main parameters varied within the following ranges: airflow rate G_b = 8.5–68.5 g s^{-1}, density of volumetric heat generation q_v = 0–4.5×10^8 W m^{-3}, heat flux q_w = 0–1.8×10^5 W m^{-2}, wall temperature T_w = 278–540 K, flow temperature T_b = 278–310 K, temperature factor T_w/T_b = 1.75, Reynolds number $Re_b = 1 \times 10^4$–8.5×10^4, rate of wall temperature change $|\partial T_w/\partial \tau|$ up to 70 K s^{-1}, rate of flow rate change $|\partial G/\partial \tau| = 4 \times 10^{-3}$–$20 \times 10^{-3}$ kg s^{-2}, and relative distance from the start of heating z/d_e = 4–50.

In order to experimentally determine the heat transfer coefficient under unsteady-state conditions

$$\alpha_{un}(z, \tau) = \frac{q_w(z, \tau)}{T_w(z, \tau) - T_b(z, \tau)} \tag{33}$$

it is necessary to know the change in time of the working fluid mean mass temperature, wall temperature and of the heat flux density on it. The values of $T_w(z,\tau)$ and $q_w(z,\tau)$ were determined from the measured temperature of the non-cooled surface of the plate $T_H(z,\tau)$ and $q_c(z,\tau)$ with allowance for heat spent to heat or cool the plate itself and for the radiant heat transfer in the channel. The values of $T_b(z,\tau)$ were found by solving a one-dimensional energy equation for the flow from the measured flow temperature at the inlet, flow rate $G(\tau)$ and calculated values of $q(z,\tau)$.

As the heat generation in the plate increases, the wall temperature increases faster, the greater z/d_e is. In this case $K_\alpha > 1$, and the difference of K_α from 1 is greater, the higher z/d_e is. At the beginning of the process $K_\alpha = 3$–4, then, as the wall temperature is stabilized, $K_\alpha \to 1$ (Fig. 9). With an increase of Re_b, the influence of the thermal unsteadiness on K_α decreases (Fig. 10).

When the heat generation in the plate decreases, the wall temperature declines faster, the higher z/d_e is. In this case $K_\alpha < 1$, with the difference of K_α from 1 being greater, the higher $|\partial T_w/\partial\tau|$ is. At the beginning of the process $K_\alpha = 0.7$–0.8 (Fig. 9).

In the absence of the segment of hydrodynamic stabilization (Section No. 1), the following correlation is obtained for the case of the wall temperature increase:

$$K_\alpha = 1+\Delta K_2 = 1+\left(\frac{460}{Re_b^{0.5}}+\frac{8.13}{Re_b^{0.46}}\frac{z}{d_e}\right)K_{Tg}\times 10^4 \tag{34}$$

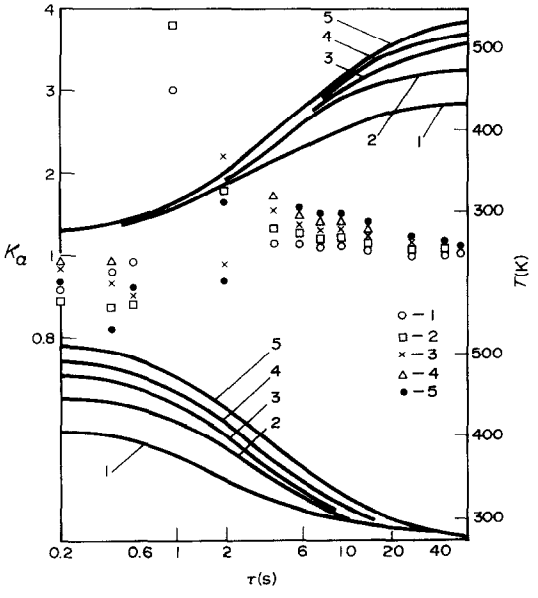

FIG. 9. Dependence of the wall temperature T_w (lines) and of the quantity K_α (points) on time on a steep increase ($K_\alpha > 1$) and a decrease ($K_\alpha < 1$) of heat loading in the wall of Test Section No. 1: 1–5, z/d_e = 10.6, 19.1, 27.7, 36.2, 44.0.

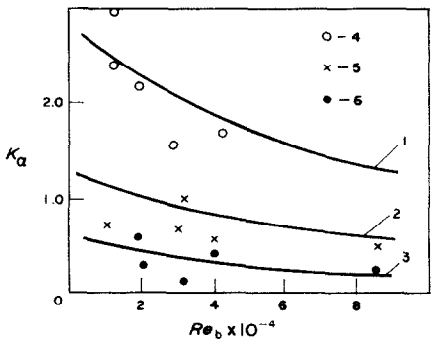

FIG. 10. Dependence of K_α on Re_b on an increase of heat loading in the plane channel wall (Section No. 1): 1–3, average relations for $K_{Tg}\times 10^4 = 0.23$, 0.11, 0.05, respectively; 4–6, experimental points for $K_{Tg}\times 10^4 = 0.21$–0.25, 0.1–0.12, 0.04–0.06.

which is valid at $Re_b = 1.0\times 10^4$–8.5×10^4; $K_{Tg} = 0$–0.22×10^{-4}; $T_w/T_b = 1$–1.75.

For the case of a decreasing wall temperature the following relation is obtained:

$$K_\alpha = \exp(0.813K_{Tg}\times 10^4) \tag{35}$$

which is valid at $Re_b = 1.0\times 10^4$–8.5×10^4; $K_{Tg} = -0.22\times 10^{-4}$ to 0; $T_w/T_b = 1$–1.75.

In the presence of the hydrodynamic stabilization segment (Section No. 2) the generalizing relations within the same ranges of the parameter K_{Tg} have the following forms:

for an increasing heat flux

$$K_\alpha = 1+\left[a+4.6\exp(-0.3Re_b\times 10^{-4})+\frac{3.9\times 10^4}{Re_b^{1.34}}\left(\frac{z}{d_e}\right)\right]K_{Tg}\times 10^4 \tag{36}$$

where $a = 1.4$–$0.2Re_b\times 10^{-4}$ when $Re_b < 2\times 10^4$; $a = 1$ when $Re_b \geq 2\times 10^4$;

for a decreasing heat flux

$$K_\alpha = \exp(0.76K_{Tg}\times 10^4). \tag{37}$$

In experiments with a varying working fluid flow rate in the channel the temperature of the electrically heated wall was kept constant with the aid of a special automatic system to exclude the influence of the tem-

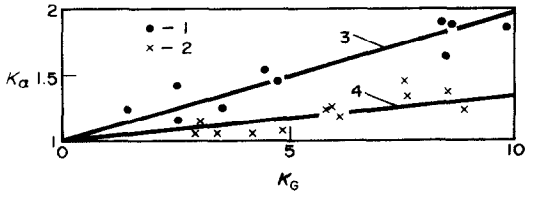

FIG. 11. The influence of Re on the dependence of K_0 on K_G for $z/d_e = 19$: 1, 2, experimental data for $Re_b\times 10^{-4} = 1$–1.5 and 3–4, respectively; 3, 4, generalizing relations for $Re_b\times 10^{-4} = 1.25$ and 3.5.

perature unsteadiness. It was found that as the flow was speeded up the non-stationary heat transfer coefficients could exceed their quasi-stationary counterparts by a factor of two, while during the deceleration of flow they could be much below their quasi-stationary values. As $|\partial G/\partial\tau|$ decreases and Re_b increases, the value of $K_\alpha \to 1$ (Fig. 11).

According to ref. [1], the influence of the hydrodynamic unsteadiness was taken into account with the aid of the dimensionless parameter

$$K_G = \frac{\partial G}{\partial \tau}\frac{d_e^2}{G\nu_b}. \quad (38)$$

For the flow rate increasing in time ($K_G > 0$) (for Section No. 1) the following generalized relation is obtained:

$$K = 1 + \Delta K_3 = 1 + \left\{8 + 44\exp\left[Re_b \times 10^{-4}(0.71 - 0.296 Re_b \times 10^{-4}) + c\frac{z}{d_e}\right]\right\} K_G \times 10^{-3} \quad (39)$$

where $c = 1.4 - 0.36 Re_b \times 10^{-4}$ when $Re_b \leqslant 3.5 \times 10^4$; $c = 0$ when $Re_b \geqslant 3.5 \times 10^4$.

For a decreasing flow rate ($K_G < 0$) the relation is

$$K_\alpha = \exp\left(\frac{0.065 K_G}{Re_b \times 10^{-4}}\right). \quad (40)$$

These relations are valid at $Re_b = 1.25 \times 10^4$–8.5×10^4; $T_w/T_b = 1$–1.75; and when $-15 > K_G > 15$. For heat transfer over the thermal initial segment (Section No. 2) with an increasing flow rate the following relation is obtained for $0 < K_G < 15$:

$$K_\alpha = 1 + \left\{\frac{74}{(B+0.1)^{0.47}} + [2.85\exp(-1.28B^2) + 0.8]\frac{z}{d_e}\right\} K_G \quad (41)$$

where $B = Re_b \times 10^{-4} - 1$. For a decreasing flow rate with $-15 < K_G < 0$ the relation is

$$K_\alpha = \exp(0.0288 K_G). \quad (42)$$

Under investigation in a plane channel were also the regimes with simultaneously varying wall temperature and working fluid rate. It was found that the simultaneous influence of the thermal and hydrodynamic unsteady states cannot be taken into account by determining the values of ΔK_2 and ΔK_3 from equations (34)–(42) and then by summarizing them as recommended in ref. [1] for a circular tube, i.e.

$$K_\alpha \neq 1 + \Delta K_2 + \Delta K_3. \quad (43)$$

Thus, the investigations showed that non-stationary coefficients of heat transfer and mixing in complex-shaped channels with turbulent flow regimes can differ substantially from quasi-stationary values and that they are determined by the rates of change of boundary conditions.

REFERENCES

1. E. K. Kalinin, G. A. Dreitser, V. V. Kostyuk and I. I. Berlin, *Methods for Calculating Conjugate Heat Transfer Problems*. Izd. Mashinostroenie, Moscow (1983).
2. L. A. Ashmantas, B. V. Dzyubenko, G. A. Dreitser and M. D. Segal, Unsteady-state heat transfer and mixing of a heat carrier in a heat exchanger with flow twisting, *Int. J. Heat Mass Transfer* **28**, 867–877 (1985).
3. B. V. Dzyubenko, M. D. Segal, L. A. Ashmantas and P. A. Urbonas, Unsteady-state mixing of a heat carrier in a heat exchanger with helical tubes, *Izv. Akad. Nauk SSSR, Energ. Transp.* No. 3, 125–133 (1983).
4. Yu. I. Danilov, B. V. Dzyubenko, G. A. Dreitser and L. A. Ashmantas, *Heat Transfer and Hydrodynamics in Complex-shaped Channels*. Izd. Mashinostroenie, Moscow (1986).
5. A. B. Bagdonavichyus and A. V. Kalyatka, Unsteady-state mixing of heat carrier in bundles of coiled tubes on a sudden change of the flow rate. In *Physical-Technical Problems of Power Engineering* (Collected Papers), pp. 168–171. Izd. IFTPE Akad. Nauk Lit. SSR, Kaunas (1986).

TRANSFERT VARIABLE DE CHALEUR ET DE MASSE DANS DES CANAUX DE FORME COMPLIQUEE

Résumé—On considère le problème du transfert thermique variable et du mélange du fluide dans des canaux formés par des grappes à assemblage serré de tubes helicoïdaux à section ovale, avec un écoulement général longitudinal et dans un canal plan avec chauffage sur un seul côté. Des champs de température variable sont calculés et des résultats expérimentaux sont donnés pour les mécanismes de transfert de chaleur et de masse dans des grappes de tubes en serpentin. On donne des nouvelles lois sur ces mécanismes. On trouve que dans les mécanismes variables les coefficients de transfert thermique et de diffusion turbulente sont significativement différents de leur correspondant quasi-stationnaire. Cette différence est déterminée par la vitesse de changement des conditions aux limites: température pariétale et vitesse du gaz refroidissant. On donne l'explication des lois obtenues aussi bien que les recommandations pour calculer le transfert thermique et le mélange variables et pour déterminer les limites d'application des valeurs quasi-stationnaires pour les coefficients de transfert thermique et de mélange.

NICHTSTATIONÄRER WÄRME- UND STOFFTRANSPORT IN KOMPLIZIERT GEFORMTEN KANÄLEN

Zusammenfassung—In diesem Beitrag wird das Problem des nichtstationären Wärmetransports und der Vermischung des Arbeitsfluids betrachtet, sowohl in Kanälen, die aus dicht gepackten Bündeln von aufgewickelten Ovalrohren mit einer Längsströmung bestehen, als auch in einem ebenen Kanal, der einseitig beheizt wird. Für die Wärme- und Stofftransportvorgänge in Bündeln aufgewickelter Rohre werden nichtstationäre Temperaturfelder berechnet und experimentelle Ergebnisse vorgestellt. Es wurden neue Gesetzmäßigkeiten gezeigt, die den Verlauf dieser Vorgänge bestimmen. Es wurde herausgefunden, daß sich die Wärmeübergangskoeffizienten bei turbulenter Diffusion in nichtstationären Prozessen wesentlich von denen im quasistationären Fall unterscheiden. Dieser Unterschied ist durch die Anzahl der Änderungen von Randbedingungen bestimmt: die Wandtemperatur und der Massenstrom des Kühlgases. Die erhaltenen Gesetzmäßigkeiten werden erläutert und Empfehlungen zur Berechnung des nichtstationären Wärmetransports und der Vermischung in Kanälen und zur Bestimmung der Anwendungsgrenzen quasistationärer Werte für die Wärmeübergangs- und Mischungskoeffizienten gegeben.

НЕСТАЦИОНАРНЫЙ ТЕПЛОМАССООБМЕН В КАНАЛАХ СЛОЖНОЙ ФОРМЫ

Аннотация—Рассматривается задача о нестационарном теплообмене и перемешивании теплоносителя в кааналах, образованных плотно упакованными продольно обтекаемыми пучками витых труб овального профля, и в плоском канале с односторонним подводом тепла. Представлены результаты расчета нестационарных полей температур и экспериментального исследования процессов тепломассопереноса в пучках витых труб. Выявлены новые закономерности протекания этих процессов. Обнаружено, что в нестационарных процессах наблюдается существенное отличие коэффициентов теплообмена и эффективных коэффициентов турбулентной диффузии от их квазистационарных значений. Это отличие определяется скоростями изменения граничных условий—температуры стенки и расхода охлаждающего газа. Даются объяснение полученных закономерностей и расчетные рекомендации, позволяющие проводить расчеты нестационарных процессов теплообмена и перемешивания в каналах и определять границы применимости квазистационарных значений для коэффициентов теплоотдачи и перемешивания.